X-Ray Interferometry of Volume Changes in C^+ Implanted Silicon *

G. H. Schwuttke and K. Brack

IBM Laboratories, Hopewell Junction, New York

(Z. Naturforsch. **28 a**, 654—656 [1973] ; received 30 Januaray 1973)

Dedicated to Professor G. Borrmann on the occasion of his 65th birthday

High energy C^+ implantation is used to construct a two crystal monolithic X-ray interferometer. The X-ray interferometer technique is applied to in-situ studies of radiation damage annealing in the interferometer. Volume changes in the crystal due to the transformation of single crystal silicon to amorphous silicon and due to the formation of silicon carbide are measured.

Introduction

The Bonse and Hart Laue X-ray interferometer consists of three Bragg reflecting wafers: The beam splitter, the mirror and the analyzer [1]. Such a device is made from a large and highly perfect single crystal block simply by cutting two wide grooves into the block. Thus different parts of the same crystal serve as beam splitter, transmission mirror, and analyzer crystal. In this way the important spatial lattice coherence between all three crystals is easily maintained over long periods of time. The function of the mirror crystal in the Laue interferometer is to make optical contact between the exit surface of the beamsplitter and the entrance surface of the analyzer crystal. This function can be eliminated by placing the beamsplitter and the analyzer crystal on top of each other, such that both crystals are making physical contact while they are simultaneously Bragg reflecting.

This technique has successfully been used to study dislocations in two crystal Moiré topographs [2]. The technique of holding two separate crystal plates in physical contact with interferometric sensitivity is difficult and requires great experimental expertise. Other bi-crystal interferometers that are simpler to operate have been described by Chikawa and Ikeno, et al. [3]. These investigators produced two crystal Moiré topographs from as-grown bi-crystals in which the two crystal parts had different lattice parameters.

Recently, the application of high energy ion implantation was shown to be an elegant way to produce a monolithic interferometer [4]. Such an interferometer was used to determine lattice strains in silicon due to ion implantation and also ion implantation depth [4]. This paper describes the application of such a bi-crystal interferometer to the study of annealing of radiation damage in silicon after high energy ion implantation.

Experimental

A two component X-ray interferometer was fabricated through high energy ion bombardment as shown schematically in Figure 1 **. Such a bi-crystal combination consists of a perfect bulk crystal and a perfect layer crystal. Both crystals are separated by a damage zone which can be completely amorphous and lens-shaped [4]. The two crystals have the same crystallographic orientation, the same lattice constant but are separated by a small rigid body displacement [4]. Thus the "feat" of holding two crystals in "physical contact" with interferometric sensitivity is easily achieved. Transmission topographs of such crystals are obtained by standard topographic techniques. The topograph of a Si wafer after 1 MeV C^+ implantation, holding 10^{15} C^+ ions/cm^2, is shown in Figure 2. X-ray interference fringes are clearly visible. The interference fringes have some unique properties [4]: (1) The number of ringes depends on the irradiation dose. (2) The number of fringes depends on the Bragg reflection. (3) The fringes are curves of constant $\boldsymbol{h}\cdot\boldsymbol{c}$ and thus contour lines of the displacement $\boldsymbol{c}$ over the beam cross-section. (4) The variation δc per fringe obeys the equation $|\delta c| = (h\cdot z)^{-1}$. (5) The maximum displacement is equal to the total number of ringes time δc.

Reprint requests to Dr. G. H. Schwuttke, Dept. 269, Build. 300-90, IBM E. Fishkill Facility, Rt. 52, *Hopewell Junction*, N. Y. 12533, U.S.A.

* This work was supported in part under Air Force Contract F19628-71-C-0095, Air Force Cambridge Research Laboratories, Bedford, Massachusetts, U.S.A.

** Figures 1—5 on page 656 a, b.

This type of monolithic two crystal interferometer allows some interesting applications. Specifically, it can be used to study the annealing of subsurface amorphous films. Such an application is described in the following section.

Measurements and Discussion

For the annealing measurements the sample shown in Fig. 2 was cut in half along the line indicated in the figure. A series of annealing experiments was performed on both halfs to determine the influence of temperature on the amorphous layer. The samples were annealed to 1200 °C most of the time in intervals of 100 °C. Each annealing cycle lasted for one hour. For each temperature the width of the subsurface damage zone was measured optically on a bevel using sample 1, and subsequently X-ray interference topographs were recorded. These measurements were supported through extensive transmission electron microscopy work combined with selected area diffraction studies. The electron microsopcy work was done on sample 2 and is reported in detail elsewhere [5].

Width of Damage Zone

The width of the subsurface damage zone was measured after every annealing cycle on a 1 or 4 degree bevel. Representative and important examples of this measurement series are shown in Figure 3. The subsurface damage zone obtained through the 1 MeV C^+ bombardment is shown in the photomicrograph of Figure 3 a. By measuring the bevel angle precisely, the position of the center of the subsurface damage layer is calculated to be 1.5 μm below the surface. Systematic electron diffraction studies of the damage zone shown in Fig. 3 a indicate that the disturbed layer consists of a continuous lens-shaped sheet of amorphous silicon [5]. The sheet reaches a maximum thickness of ~3000 Å. It is interesting to not that up to 500 °C the damage width stays fairly constant. The damage zone obtained after the 500 °C one hour anneal is shown in Figure 3 b. At 600 °C the width of the amorphous zone starts to decrease (Figure 3 c). In general we find about half the thickness of the amorphous layer after the 600 °C anneal. The decrease in damage width was correlated with the start of crystallization of the amorphous layer [5]. The auto-epitaxial crystallization of the amorphous zone is completed after a one hour anneal at 700 °C. Thereafter, the damage zone is not visible anymore on the bevel. This is shown in Fig. 3 d which represents the disturbed zone after a 700 °C heat treatment. The original position of the amorphous zone is indicated on the photomicrograph of Figure 3 d. After a one hour anneal at 1200 °C the buried layer is again visible at a depth of 1.5 μm. This is shown in the photomicrograph of Figure 3 e.

X-Ray Interference Topography

All changes that occur in the damage zone as described in connection with Fig. 3 are readily observed non-destructively with the two crystal interferometer. A sequence of X-ray interference topographs obtained from the sample shown in Fig. 3 is given in Figure 4. Note the reduction in the number of fringes from 13 in the sample as bombarded (Fig. 2) down to two fringes after the 800 °C anneal cycle (Figure 4 c). After the 900 °C anneal the trend is reversed and three fringes are visible. Additional annealing at higher temperatures causes additional changes in the interference pattern which finally stabilizes at 1200 °C where four fringes are visible.

A quantitative evaluation of the annealing through X-ray interference fringe changes is possible. As shown previously [4], one fringe change corresponds to 5.4 Å (111 reflection and (100) crystal orientation, Mo$K\alpha$-radiation). Therefore, 13 fringes as counted after bombardment (Fig. 1 b) indicate an expansion of ~70 Å. This is approximately 2.3% of the total damage zone measured to be approximately 3000 Å wide after implantation (Figure 3 a). Consequently, amorphous silicon occupies a volume approximately 2% to 3% larger than single crystal silicon.

The interference technique reveals not only that annealing of the sample to 800 °C reduces the number of fringes from originally 13 down to only 2 in agreement with the volume reduction accompanying the crystallization of the amorphous damage zone but also that higher annealing results again in a volume expansion of the damage zone. New fringes appear after 900 °C annealing until after 1200 °C annealing a maximum number of 4 fringes is achieved. It was shown that this volume expansion accompanies silicon carbide formation that starts at 900 °C and is completed after the 1200 °C anneal [5]. Thus X-ray interferometry is also a useful technique in recognizing second phase formation in ion implanted silicon. This technique was successfully used to fabricate subsurface insulating films of silicon nitride in silicon [6].

[1] U. Bonse and M. Hart, Appl. Phys. Lett. **6**, 155 [1965] and Appl. Phys. Lett. **7**, 99 [1965].
[2] A. R. Lang and V. F. Minscov, Appl. Phys. Lett. **7**, 214 [1965].
[3] J. I. Chikawa, Appl. Phys. Lett. **7**, 193 [1965].
[4] U. Bonse, M. Hart, and G. H. Schwuttke, Phys. Stat. Sol. **33**, 361 [1969].
[5] K. Brack, E. Gorey, and G. H. Schwuttke, Radiation Effects to be published December 1972.
[6] G. H. Schwuttke and K. Brack, Trans. Met. Soc. AIME **245**, 475 [1969].

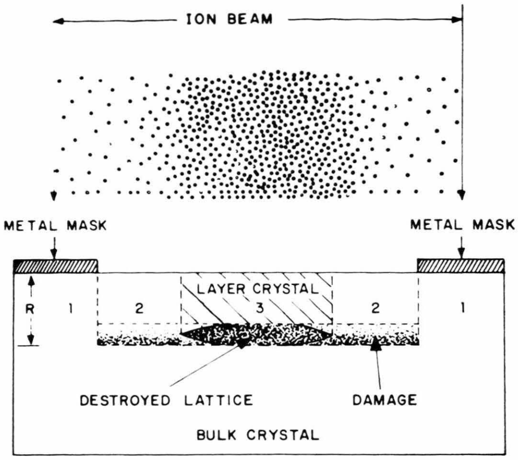

Fig. 1. Schematic of two component X-ray interferometer produced by high energy ion implantation.

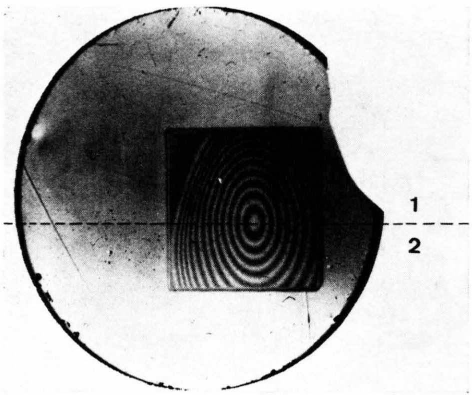

Fig. 2. Transmission topograph of perfect silicon slice after 1 MeV C^+ bombardment. Note interference fringes.

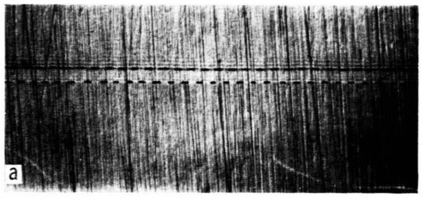

Fig. 3 a

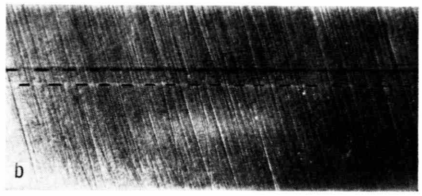

Fig. 3 b

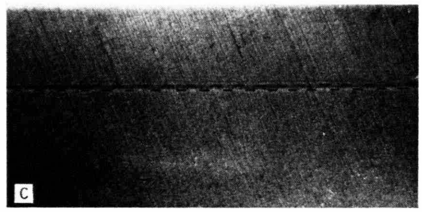

Fig. 3 c

Fig. 3 d

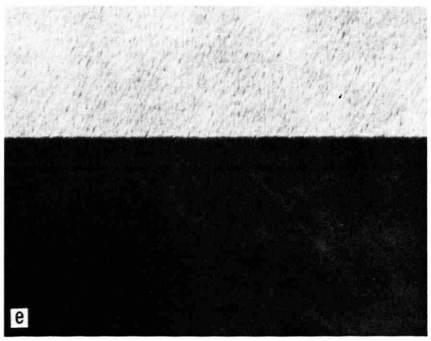

Fig. 3 e

Fig. 3 a—3 e. Photomicrographs showing damage zone on a bevel after 1 MeV C^+ bombardment. Bevel angles are about 1 or 4 degrees. The depth of the layer is 1.5 μm below the surface.
a) No anneal. b) After 500 °C anneal. c) After 600 °C anneal. d) After 700 °C anneal. e) After 1200 °C anneal.

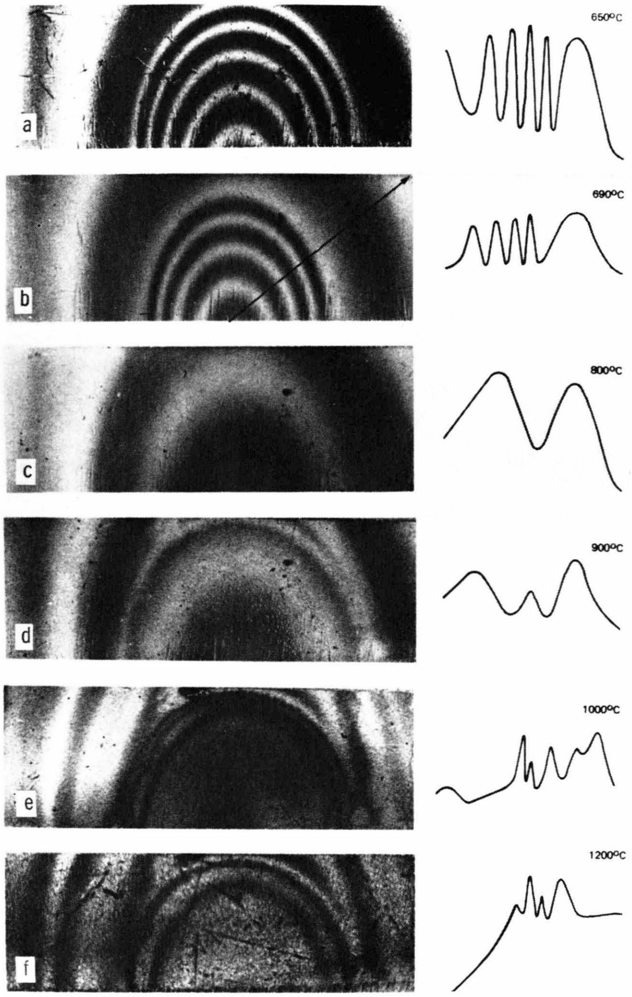

Fig. 4 a

Fig. 4 b

Fig. 4 c

Fig. 4 d

Fig. 4 e

Fig. 4 f

Fig. 4 a—4 f. Sequence of interference topographs of wafer shown in Fig. 3 recorded at different annealing cycles shown at right (MoKα radiation, 111 recording). The direction of the photodensitometer scan (on the left) for all interference topographs is indicated by the arrow in 4 b.